Suplemento de la Revista Mexicana de Física **2** (1) 66–71 JANUARY-MARCH 2021

Fiber laser refractometer operating in the 2 μm spectral region based on the MMI effect

O. Gaspar-Ramírez

Universidad Autónoma de Nuevo León,
San Nicolás de los Garza 66455, México;
e-mail: omar.gasparrm@uanl.edu.mx

R. I. Álvarez-Tamayo

Universidad Popular Autónoma del Estado de Puebla,
Puebla 72410, México;
e-mail: ricardoivan.alvarez01@upaep.mx

P. Prieto-Cortés

Universidad Autónoma de Nuevo León,
San Nicolás de los Garza 66455, México.
e-mail: patricia.prietocts@uanl.edu.mx

M. Durán-Sánchez

Conacyt-Instituto Nacional de Astrofísica, Óptica y Electrónica,
L. E. Erro 1, Puebla 72824, México.
e-mail: mduransa@conacyt.mx

Received 13 November 2020; accepted 21 December 2020

We experimentally demonstrate a fiber laser refractometer based on the use of a multimode interference (MMI) fiber structure. The MMI filter is constructed with an uncladded fiber segment, which acts as a sensing element to determine the refractive index (RI) of liquid solutions. The laser emission, generated at the 2 μm waveband, is wavelength shifted in linear proportion to the liquid RI. The proposed fiber laser refractometer exhibits a high sensibility of 937.81 nm/RIU.

Keywords: Fiber laser; sensor; refractometer; multimode interference.

PACS: 2.85.Hz; 42.55.Wd; 07.07.Df

1. Introduction

Thulium-doped fiber lasers (TDFLs) have been of great interest due to their many potential applications. TDFLs operate in the eye-safe spectral window, from 1.8 to 2 μm, which makes them attractive for application in non-invasive surgery, remote sensing of atmospheric CO_2 and H_2O, LIDAR, free-space communications, and characterization of thulium-doped fiber amplifiers [1-5]. Tunable TDFLs have been reported in optical sensing approaches for remote sensing and gas detection for different absorption peaks whose absorption wavelengths lies within the emission range of the thulium-doped fiber (TDF), used as a gain medium [6-8]. The outstanding advantages of using fiber laser systems in optical sensing include real-time measurements, compactness and robustness, stability, and electromagnetic immunity, among others.

In order to obtain wavelength tuning in fiber lasers, spectral filters such as high-birefringence optical loop mirrors [9,10], fiber Bragg gratings (FBG) [11,12], Mach-Zehnder interferometers [13], fiber tapers [14], polarization variation devices [15] are commonly used. In this regard, wavelength filters based on multimodal interference (MMI) [16-18] exhibit advantages, compare to other filters, for their use in laser wavelength tuning due to its low cost, easy construction, and compactness, compared to other filters [19]. Additionally, MMI filters have been used for the generation of multiple laser wavelengths [20]. The operation principle of an MMI filter is based on the self-imaging effect, described by Soldano in Ref. [21], for a single-mode-multimode-single-mode (SMS) waveguide structure. Because MMI filters exhibit high sensitivity to different physical quantities, they have received attention for their use as sensing element in the development of fiber-based optical sensors for measurement of temperature [22,23], curvature [24,25], biological markers [26], and vibration [27]. In this sense, fiber-based refractometers have been of great interest in technological and biological areas [28-30]. Their advantages include high sensitivity, fast response time, immunity to electromagnetic interference, and chemical neutrality [30].

In this paper, we experimentally demonstrate a fiber laser refractometer based on a tailored MMI filter as a sensing element inserted within a ring cavity thulium-doped fiber laser. The operation of the TDFL in a wavelength range near the 2 μm wavelength region allows sensing of liquid refractive index (RI) by laser wavelength displacement in an extended

waveband of around 100 nm. The SMS fiber structure uses an uncladded fiber (UCF) as multimode fiber (MMF) segment of the MMI filter, then, when it is submerged into the liquid, the surrounding medium acts as UCF cladding, which leads to a wavelength tuning of the laser line, proportional to the RI of the liquid in a wavelength range from 1957.3 to 1987.3 nm, for RI variations in a range from 1.4 to 1.432. The sensibility of the refractometer is 937.81 nm/RIU.

2. Design and construction of the MMI filter

The MMI fiber structure consists of a UCF segment spliced between SMF segments, as is shown in Fig. 1. The operation principle of the MMI fiber filter is based on the self-imaging effect. The single mode of light traveling through the input SMF extends, causing high order modes when reaches the UCF segment. The multiple modes through the UCF length interfere with each other, resulting in individual and periodic images where the UCF behaves as the MMF of the structure in which the surrounding medium acts as cladding. The generation of the self-images occurs at specific physical lengths of the UCF where the maximum modes of interference is obtained [21]. The central wavelength λ_0 for the maximum interference are the self-image p, which occurs at the UCF physical length L, depends on the UCF effective RI n_{UCF} and its diameter D_{UCF}, as follows:

$$\lambda_0 = p\frac{n_{UCF}D_{UCF}^2}{L}, \tag{1}$$

then, the length L of the UCF is calculated in order to match the self-image at the fiber structure length where the splice between the UCF and the output SMF is reached by the traveling modes. Thus, for the obtained UCF fiber length, the maximum interference peak is exhibited at the convenient central wavelength.

The MMI fiber structure was constructed with a UCF segment with RI of 1.463, a diameter of 125 μm and length of $\sim$4.5 cm, to obtain the central peak wavelength of the transmission spectrum near 1900 nm wavelength region for the fourth self-image interference.

3. Experimental setup

The fiber laser refractometer is based on the use of a ring cavity TDFL. The experimental setup is shown in Fig. 2. The laser cavity includes a 2 m long segment of single-mode double-clad TDF (Nufern, SM-TDF-10P/130-HE), used as

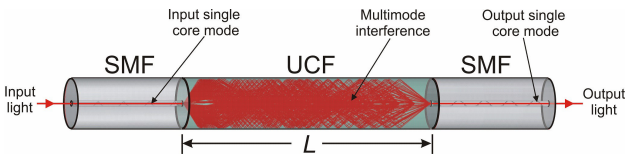

FIGURE 1. Schematic of the MMI fiber filter.

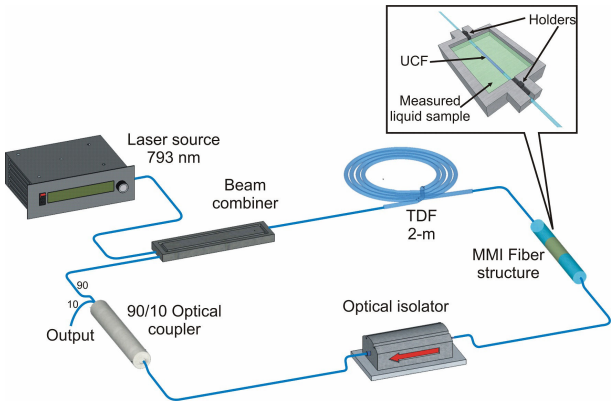

FIGURE 2. Experimental setup of the fiber laser refractometer.

a gain medium. The TDF with a first cladding absorption coefficient of 3 dB/m at 793 nm, (first cladding diameter and numerical aperture (NA) of 130 μm and 0.46; core diameter of 10 μm and core NA of 0.15) is cladding pumped by a 10 W multimode laser source at 793 nm through a $(2+1)\times 1$ beam combiner. The MMI filter used as an RI sensing element is inserted between the TDF and an optical isolator, which ensures the unidirectional light propagation. A 90/10 optical coupler closes the ring cavity. The 10% port of the optical coupler is used as the output port. An optical spectrum analyzer (OSA) with maximal resolution of 0.05 nm is connected to the output port to measure the transmitted spectrum of the MMI filter and the output laser spectrum; and an optical power meter for measurement; of the laser output power.

The MMI fiber structure is mounted on a mechanical device, which allows submersion of the UCF segment under the liquid sample to be measured. A couple of holders fixes the fiber position. The liquid surrounding the UCF acts as cladding whose RI modifies the effective width of the propagated modes. As a consequence, the effective RI is also modified, then, the central wavelength of the MMI transmission peak shifts in proportion to the RI of the liquid, as it can be expected from Eq. (1) [21].

4. Results and discussion

The transmission optical spectrum of the MMI filter was measured by using the amplified spontaneous emission (ASE) of the TDF as input source. For this purpose, the laser cavity was opened at the splice between the 90% output port of the optical coupler and the input signal port of the beam combiner. Figure 3a) shows the optical spectrum of the TDF ASE and the optical spectrum of the MMI filter transmission measured at the output port with the OSA. The measurements were obtained with a pump power level of 1.4 W. The inset of Fig. 3a) shows the transmission of the MMI filter exposed to air, obtained as the division of the measured MMI transmitted optical spectrum by the TDF ASE optical spectrum. As it can be observed, the central transmission wavelength is 1930 nm, the full width at half maximum (FWHM) bandwidth is

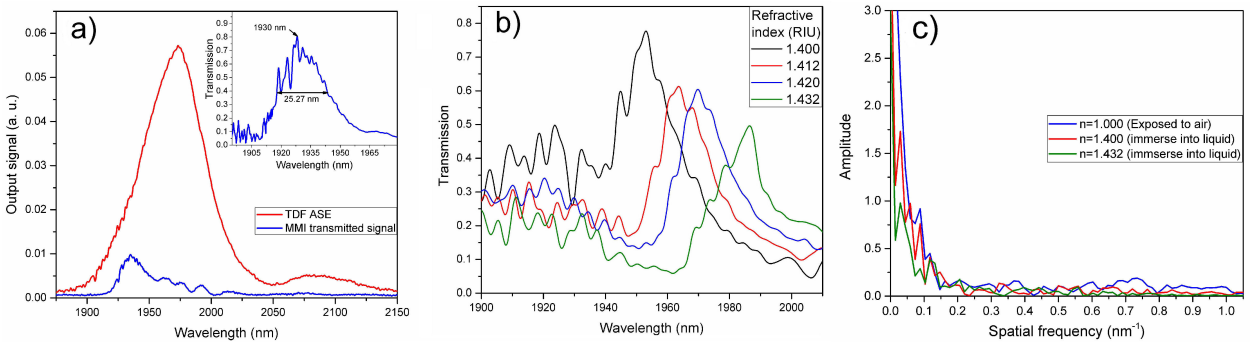

FIGURE 3. Characterization of the MMI filter: a) Spectrum of the TDF ASE input source and of the MMI filter transmitted spectrum, inset: Transmission of the MMI spectrum exposed to air ($n = 1$), b) transmission spectra of the MMI filter for RI variations of liquid, c) comparison of FFT-spatial frequency spectra for $n = 1$, $n = 1.4$, and $n = 1.432$.

25.27 nm, and the estimated insertion losses are $\sim$19%. The transmission spectrum of the MMI filter for different liquid refractive indexes is shown in Fig. 3b). The transmission spectrum of the MMI filter displaces toward longer wavelengths as the RI of the liquid increases. Besides as the transmission spectrum of the MMI filter shifts toward longer wavelengths, it can be observed an increase of insertion loss which can be attributed to the leak of high order modes due to the increase of RI of the surrounding medium, near to the RI of the UCF. Figure 3c) shows the FFT-spatial frequency spectra corresponding to the transmission spectra for the MMI exposed to air ($n = 1$) and for the minimum and maximum RI for the MMI immersed on the liquid ($n = 1.4$ and $n = 1.432$, respectively). From the FFT of the transmission spectra, it can be noticed that each transmission spectrum is constructed by the superposition of multiple interfering modes. When the

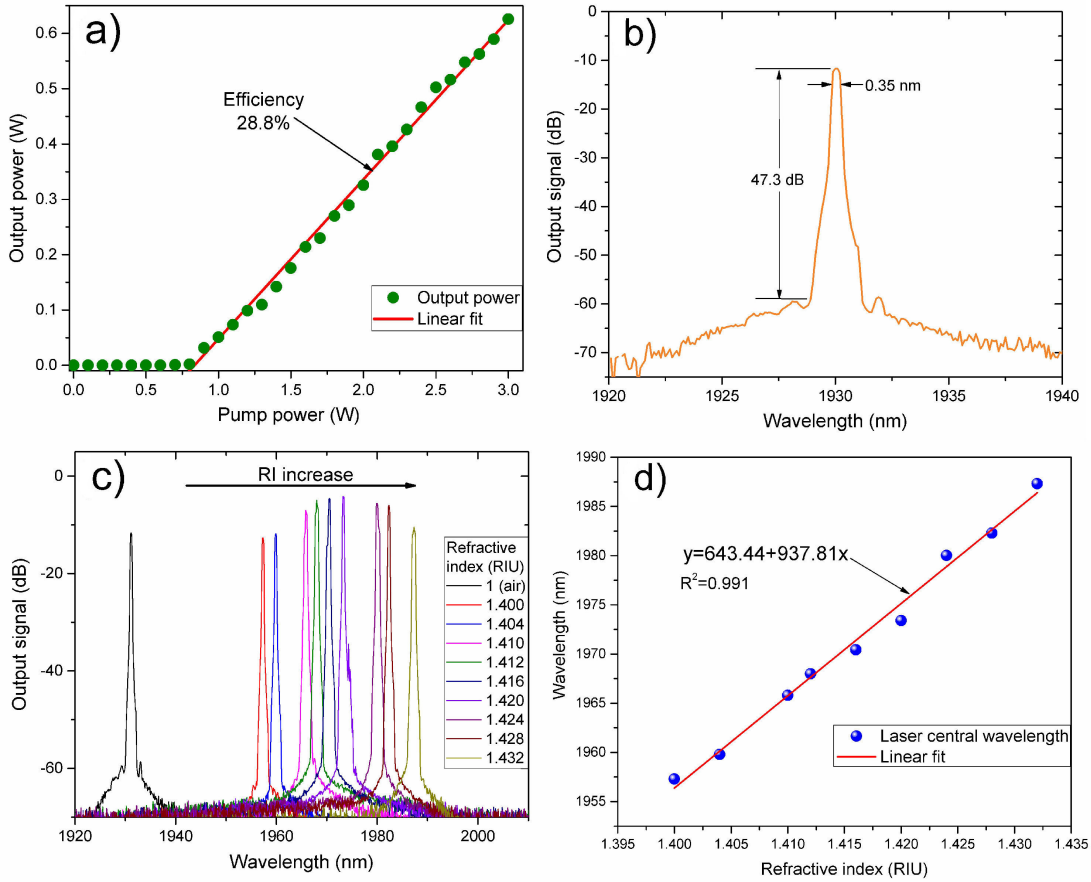

FIGURE 4. Characterization of the laser refractometer: (a) Laser efficiency, (b) output laser spectrum for MMI filter at the air, (c) output laser optical spectra for liquid solutions with different refractive indexes, (d) response of the laser emission wavelength to RI variations of different liquid solutions.

refractive index of the surrounding medium increases, some high-order modes leak to the surrounding medium leading to a lower contribution of these modes to the interference. As it can be observed, the amplitude of the dominant modes decreases, whereas the modes with weak contribution vanish, causing the increase of the insertion losses, as is confirmed by the FFT-spatial frequency spectra.

As it can be observed in Fig. 3b) when a broadband source (ASE of the TDF) is used as an input signal for the MMI fiber structure, the wavelength displacement of the transmission spectrum due to the RI variations is observable; however, a reference wavelength such as the central wavelength of the spectrum is difficult to determine leading to inconsistency on the RI sensing. In this regard, the use of a laser source significantly narrows the output spectrum allowing a more efficient interrogation method by improving the determination of a central wavelength that shifts proportionally with the variation of the refractive index of the surrounding medium. The central wavelength of the maximum transmission peak of the MMI filter shown in Fig. 3b) determines the wavelength of the laser emission when the cavity is closed.

Figure 4(a) shows the characterization of the laser output power as a function of the provided pump power. The measurements were obtained by the optical power meter at the output port with the MMI fiber structure exposed to air. The maximum output power of 625.5 mW was obtained with a pump power level of 3 W. The lasing threshold is reached with a pump power of 0.8 W. From the obtained results, the

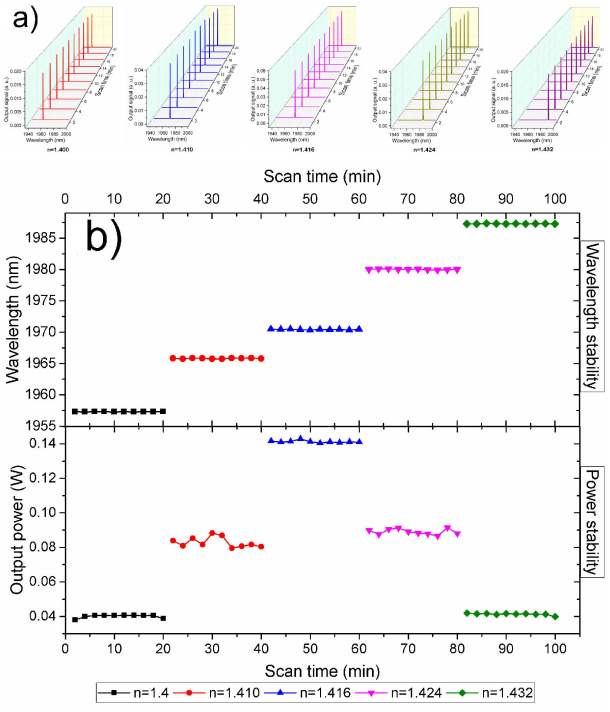

FIGURE 5. Stability of the refractometer laser emission: a) Optical spectra of the measurement sets for different refractive indexes in a time window of 20 minutes, b) wavelength and power stability of the measurement sets.

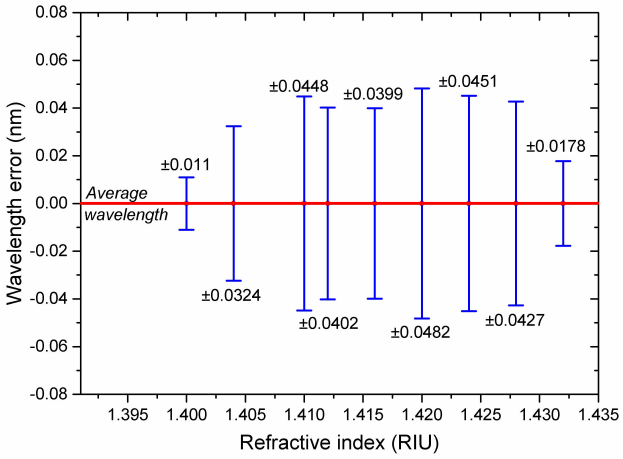

FIGURE 6. Repeatability of the refractive index sensing by wavelength displacement of the laser central wavelength.

estimated efficiency slope is 28.8%. Based on the operation principle of the proposed laser refractometer, the determination of the liquid refractive index does not require high laser output power. Then, for the characterization of the fiber laser refractometer, the pump power was fixed at 1.4 W for the stable laser output power of ∼110 mW, which, in addition, allows to avoid damage of the fiber components and the measurement instruments. The output spectrum of the laser emission is shown in Fig. 4b). The measurements were obtained with the OSA at the output port for the MMI filter exposed to air ($n = 1$). The laser line exhibits an optical signal-to-noise ratio (OSNR) of 47.3 dB and -3 dB bandwidth of 0.35 nm. The generated laser line is wavelength displaced depending on the RI of the MMI filter surrounding media. Figure 4c) shows the output laser spectra for measurements of liquid solutions with different RI in contact with the MMI filter. The RI of the liquids is in a range from 1.4 to 1.432. As it can be observed, the laser line is wavelength shifts toward longer wavelengths as the RI of the liquid increases in a wavelength range from 1957.3 to 1987.3 nm. Figure 4d) shows the central wavelength of the laser emission as a function of the RI of the liquid that can be linearly fitted to a sensitivity of 937.81 nm/RIU.

In order to investigate the stability of the laser emission for the optical refractometer, a set of ten measurements of the optical spectrum was recorded for a single measurement every two minutes in a time window of 20 minutes. The procedure was performed for a different liquid refractive index of 1.4, 1.41, 1,416, 1,424, and 1.432. The optical spectra of the five measurement sets in linear scale are shown in Fig. 5a). As it can be noticed, no significant amplitude fluctuations are observed; however, in order to perform a more detailed analysis, the output power for each measurement was simultaneously obtained by using an optical power meter. Figure 5(b) shows the wavelength and optical power stability where the central wavelength of the laser emission was obtained from the measured optical spectrum, whereas the optical power from the optical power meter recording. From the results, the

high wavelength stability of the laser emission is noticed. The maximum wavelength fluctuation of 0.068 nm was observed for liquid the RI of 1.424. For the output power stability, the maximum fluctuation of 4.1 mW, observed for the liquid RI of 1.410, represents 6.1% of the averaged output power.

To investigate the repeatability of the laser wavelength shift by RI variations on the liquid surrounding, a sequential set of ten optical spectra measurements from the lower to the higher liquid refractive index were carried out. The repeatability of measurement is shown in Fig. 6 as the calculated mean absolute error (MAE) from the average central wavelength for each tuned laser wavelength due to the liquid RI. For each liquid RI, the MAE is denoted at the corresponding error bar position. The worst-case error observed over the testing wavelengths is ± 0.482 nm (near the OSA resolution), obtained for an average central wavelength of 1965.8 nm corresponding to a surrounding liquid RI of 1.420.

As a consequence of the use of TDF as laser gain medium, the measured laser wavelengths expands in a large wavelength range, which corresponds to the amplification spectrum allowed by the TDF, over 100 nm (see Fig. 3a)), leading to an increase in the sensibility of the laser sensor.

5. Conclusions

In this work, a laser refractometer based on the use of TDF as the gain medium and a MMI filter used as a sensing element was experimentally demonstrated. The laser line is wavelength shifted proportionally to the RI of the liquid solution in contact with the UCF of the MMI fiber structure. The sensibility of the refractometer is 937.81 nm/RIU. The experimental results for RI measurements were obtained in a range from 1.4 to 1.432, which leads to laser wavelength displacements from 1957.3 to 1987.3 nm. The proposed setup has been demonstrated as a reliable and straightforward optical system for the determination of RI in liquid solutions.

Acknowledgements

R.I.A.-T was supported in part by *Fondo de Investigación UPAEP 2020* project. O.G.-R. wants to thank the CONACyT postgraduate scholarship, grant no. 817293. P.P.-C. wants to thank the CONACyT postgraduate scholarship, grant no. 160540.

1. N. M. Fried and K. E. Murray, *J Endourol*, **19** (2005) 25. https://doi.org/10.1089/end.2005.19.25
2. I. Mingareev, F. Weirauch, A. Olowinsky, L. Shah, P.Kadwani and M. Richardson *Opt. Laser Technol.*, **44** (2012) 2095-2099. https://doi.org/10.1016/j.optlastec.2012.03.020
3. T. M Taczak. and D. K. Killinger, *Appl. Opt.*, **37** (1998) 8460-8476. https://doi.org/10.1364/AO.37.008460
4. K. Scholle, E. Heumann and G. Huber, *Laser Phys. Lett.*, **1** (2004) 285. https://doi.org/10.1002/lapl.200410067
5. Z Li, A. M. Heidt, J. M. O. Daniel, Y. Jung, S. U. Alam and D. J. Richardson, *Opt. Express*, **21** (2013) 9289. https://doi.org/10.1364/OE.21.026450
6. N. P. Barnes, B. M. Walsh, D. J. Reichle and R. J. DeYoung, *Opt. Mater.*, **31** (2009) 1061. 10.1109/2944.649549
7. F. J McAleavey, J. O'Gorman, J. F. Donegan, B. D. MacCraith, J. Hegarty and G. Mazé, *IEEE J. Sel. Top. Quant.*, **3** (1997) 1103. https://doi.org/10.1364/AO.52.003957
8. K. Bremer, A. Pal, S. Yao, E. Lewis, R. Sen, T. Sun and K. T. V. Grattan, *Appl. Opt.*, **52** (2013) 3957. https://doi.org/10.1364/AO.53.004382
9. X. Ma, S. Luo and D. Chen, *Appl. Opt.*, **53** (2014) 4382. https://doi.org/10.1364/OL.35.002388
10. T. Wang, W. Ma, P. Zhang, Q. Jia, J. Zhang and H. Jiang, *J. Opt.*, **44** (2015) 210. DOI:10.1007/s12596-015-0264-7
11. F. Wang, D. Shen, D. Fan and Q Lu, *Opt. Lett.*, **35** (2010) 2388. DOI:10.1109/ACCESS.2019.2944168
12. L. Zhang, F. Yan, T. Feng, W. Han, Y. Bai, Z. Bai, and Y. Suo, *Opt. Laser Technol.*, **120** (2019) 105707. DOI:10.1109/ACCESS.2019.2944168
13. H. Ahmad, A. S. Sharbirin, A. Muhamad, M. Z. Samion and M. F. Ismail, *Laser Phys.*, **27** (2017) 065104. https://doi.org/10.1088/1555-6611/aa6bd8
14. M. V. Hernández-Arriaga *et al., J. Opt.*, **19** (2017) 115704. https://doi.org/10.1088/2040-8986/aa8d03
15. P Liu, T. S. Wang, P. Zhang, Y. Zhang, W. Z. Ma, Y. W. Su and H. L. Jiang, *Microw. Opt. Technol. Lett.*, **58** (2016) 1540. https://doi.org/10.1002/mop.29846
16. X. Ma, D. Chen, Q. Shi, G. Feng and J. Yang, *J Ligthwave Technol.*, **32** (2014) 3234. DOI:10.1109/JLT.2014.2342251
17. P. Zhang, T. Wang, W. Ma, K. Dong and H. Jiang, *Appl. Opt.*, **54** (2015) 4667. https://doi.org/10.1364/AO.54.004667
18. B. Ibarra-Escamilla *et al., Laser Phys.*, **28** (2018) 095107. https://doi.org/10.1088/1555-6611/aacb4f
19. A. Mehta, W. Mohammed and E. G. Johnson, *IEEE Photonics Technol. Lett.*, **15** (2003) 1129. DOI:10.1109/LPT.2003.815338
20. H. Ahmad, A. S. Sharbirin, M. Z. Samion and M. F. Ismail, *Appl. Opt.*, **56** (2017) 5865. https://doi.org/10.1364/AO.56.005865
21. L. B. Soldano and E. C. Pennings, *J Lightwave Technol.*, **13** (1995) 615. DOI:10.1109/50.372474
22. J. C. Aguilar-Soto, J. E. Antonio-López, J. J. Sánchez-Mondragón and D. A. May-Arrioja, *J. Phys. Conf. Ser.*,

274 (2011) 012011. https://doi.org/10.1088/1742-6596/274/1/012011

23. A. M. Hatta, G. Rajan, Y. Semenova and G. Farrell *Electron. Lett.*, **45** (2009) 1069. https://doi.org/10.1364/AO.49.000536
24. Y. Gong, T. Zhao, Y. J. Rao and Y. Wu, *IEEE Photonics Technol. Lett.*, **23** (2011) 679. Doi:10.1109/LPT.2011.2123086
25. Y. Qi, Z. Kang, Z. and S. Jian, *IEEE Sens. Lett*, **14** (2014) 1514. https://doi.org/10.1364/AO.53.006382
26. X. Li, D. Liu, R. Kumar, W. P. Ng, Y. Q. Fu, J. Yuan and Y. Semenova, *Meas. Sci. Technol.*, **28** (2017) 035105. https://doi.org/10.1088/1361-6501/aa577d
27. Y. Ran, L. Xia, Y. Han, W. Li, J. Rohollahnejad, Y. Wen and D. Liu, *IEEE Photonics J.*, **7** (2015) 1. DOI:10.1109/JPHOT.2015.2408436
28. H. Fukano, T. Aiga and S. Taue, *Jpn. J. Appl. Phys*, **53** (2014) 04EL08. https://doi.org/10.7567/JJAP.53.04EL08
29. L. Ma, Y. Qi, Z. Kang, Y. Bai and S. Jian, *Opt. Laser Technol.*, **57** (2014) 96. https://doi.org/10.1364/AO.53.006382
30. P. Chen, X. Shu, F. Shen and H. Cao, *Opt. Express*, **25** (2017) 29896. https://doi.org/10.1364/OE.25.029896